JOURNAL OF THERMOPHYSICS AND HEAT TRANSFER
Vol. 8, No. 3, July–Sept. 1994

Effects of Turbulator Profile and Spacing on Heat Transfer and Friction in a Channel

M. E. Taslim*
Northeastern University, Boston, Massachusetts 02115
and
S. D. Spring†
General Electric Aircraft Engines, Lynn, Massachusetts 01910

Turbulators in cooling passages of small turbine blades often have geometric constraints placed upon them due to casting limitations associated with small dimensions. Problems such as core die wear, cavity fill imperfections, and casting tolerance variations change turbulator profiles in their final form. This change of turbulator geometry affects, often in the wrong direction, the heat transfer coefficient and friction factor in the cooling cavity. Liquid crystals are used in this experimental investigation to study the effects of turbulator profile and spacing on heat transfer coefficient. Friction factors are also measured, and both heat transfer and friction factor results for 15 turbulator geometries are compared. For all test configurations, the turbulators are positioned on two opposite walls of a rectangular test section in a staggered arrangement with an angle of attack to the mainstream flow, $\alpha = 90$ deg. A range of turbulator blockage ratios e/D_h, pitch-to-height ratios S/e, and Reynolds numbers are tested. It is concluded that while turbulators with aspect ratios (AR_t = turbulator height/turbulator width) greater than unity produce higher heat transfer coefficients at the expense of higher pressure losses, trapezoidal-shaped turbulators, spaced properly, are very effective in heat removal with moderate pressure losses. Low aspect ratio ($AR_t < 1$) turbulators, especially with round corners, produce lower heat transfer coefficients. Furthermore, an optimum pitch-to-height ratio for 90-deg square turbulators is found to be around 8.

Nomenclature

AR = passage aspect ratio, a/b
AR_t = turbulator aspect ratio, e/w
a = nonturbulated sidewall height
b = turbulated sidewall width
D_h = hydraulic diameter based on nonturbulated cross section
EF = enhancement factor, Nu/Nu_s
e = turbulator (rib) height
$\bar{f}$ = Darcy friction factor $[\Delta P(D_h/L)/\frac{1}{2}\rho U_m^2]$
L = length of the turbulated section of the channel
Nu = Nusselt number on a turbulated wall, based on D_h
Nu_s = Nusselt number in a smooth passage, based on D_h
Pr = Prandtl number
Re = Reynolds number, based on D_h
S = turbulator pitch, center-to-center
U_m = air mean velocity
w = turbulator width
X = distance between camera and test section entrance
α = angle of attack
ΔP = pressure drop across the turbulated portion of the test section

Introduction

VARIOUS methods have been developed over the years to keep turbine blade temperatures below critical levels. The main objective in turbine blade cooling is usually to achieve maximum heat transfer coefficients while minimizing the coolant flow rate.

One such method is to route coolant air through turbulated serpentine passages within the airfoil and convectively remove heat from the blade. The coolant is then ejected either at the tip of the blade, through the cooling slots along the trailing edge or cooling holes along the airfoil surface.

Geometric parameters such as AR, turbulator height to passage hydraulic diameter or blockage ratio e/D_h, angle of attack, the manner in which the turbulators are positioned relative to one another (in-line, staggered, crisscross, etc.), turbulator pitch-to-height ratio S/e, and turbulator shape (round vs sharp corners, fillets, AR_t, skewness towards the flow direction) have pronounced effects on both local and overall heat transfer coefficients. Some of these effects were studied by different investigators and the interested reader is referred to the works of Burggraff,[1] Chandra and Han,[2] Chandra,[3] Han et al.,[4–6] Mayle,[7] Metzger et al.,[8] and Taslim et al.[9,10]

The casting process employed in the manufacture of turbine blades puts severe limitations on the size and shape of turbulators, especially in small engines. These limitations stem from a wide range of problems associated with the casting of very small turbine blades, including the inability of the molten materials to properly fill the grooves forming the final turbulators. To avoid "nonfill," the desirable tall and thin turbulators are replaced by short and fat (low aspect ratio) ones, therefore creating a cavity that is easier to fill. However, this results in severe deterioration in the heat transfer coefficients on the wall surface between turbulators. In addition to the nonfill problem, dimensional tolerances alone represent a significant deviation in heat transfer behavior for turbulators in small airfoils. As blade dimensions in modern small engines are reduced, turbulator dimensions must follow suit. However, there is a minimum practical limit to turbulator size (0.010 in.). There is also a minimum limit to the associated dimensional tolerances (0.002–0.003 in.). Thus, it can be seen that for a turbulator with a blueprint height of $e = 0.010 \pm 0.003$ in., the turbulator height can vary $\pm 30\%$. For a small airfoil, where a 0.010-in. turbulator represents a high blockage ratio, $\pm 30\%$ in turbulator height can yield significant variations in the heat transfer coefficient.

Received July 10, 1991; revision received Nov. 29, 1993; accepted for publication Jan. 6, 1994.
*Professor of Mechanical Engineering. Member AIAA.
†Staff Engineer. Member AIAA.

Table 1 Specifications

Test	e	w	S/e	e/D_h	AR	AR_t	Remarks
1	0.5	0.5	5	0.235	0.55	1	Sharp corners
2	0.5	0.25	5	0.235	0.55	2	Sharp corners
3	0.44	0.44	5	0.22	0.5	1	Sharp corners
4	0.44	0.44	7.5	0.22	0.5	1	Sharp corners
5	0.44	0.44	10	0.22	0.5	1	Sharp corners
6	0.5	0.5	5	0.235	0.55	1	Round corners and fillets
7	0.5	0.25	5	0.235	0.55	2	Round corners and fillets
8	0.5	0.375	5	0.235	0.55	1.33	Trapezoidal
9	0.57	0.57	7.7	0.285	0.5	1	Max tolerance
10	0.31	0.57	14.2	0.155	0.5	0.55	Min tolerance
11	0.585	0.585	4.27	0.275	0.55	1	Max tolerance
12	0.44	0.585	5.68	0.207	0.55	0.77	Min tolerance
13	0.36	0.25	6.94	0.17	0.55	1.45	Round corners and fillets
14	0.3	0.3	10	0.15	0.5	1	Round top corners
15	0.3	0.48	10	0.15	0.5	0.625	Round top corners

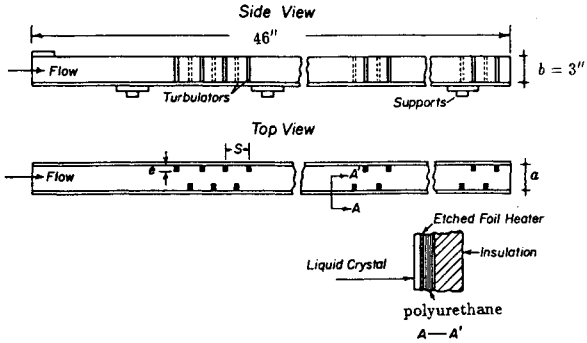

Fig. 1 Layout of a typical test section.

Another problem facing the designer of these cooling cavities is the gradual wearing of the core die. Relatively sharp-edged turbulators with small fillets, cast at the beginning of a core die life span, eventually deteriorate to rounded corner turbulators with large fillets as the die wears. This change in turbulator profile will affect the flow pattern, which in turn decreases the heat transfer performance of the turbulator accompanied with a decrease in the pressure drop. Turbulator pitch-to-height ratio S/e is another important parameter that deserves careful consideration. Since a turbulated cooling passage approaches the all-smooth-wall channel at the upper and lower bounds ($S/e \rightarrow 0$ and $S/e \rightarrow \infty$), there exists an optimum value for S/e at which the passage has the best heat transfer performance. The influence of S/e on heat transfer behavior becomes more significant when it is realized that as turbulator height decreases (due to die wear), S/e increases. Hence, as turbulator height decreases, S/e is changing either towards or away from its optimum.

This investigation will report on relative differences in heat transfer behavior due to geometrical changes (specifically S/e and turbulator shape) that typically occur in small cast airfoils. Because of the difficulties encountered when casting turbulators in small airfoils, and the resultant potential change in heat transfer behavior associated with nonideal turbulators, there exists a need to understand the impact these changes have.

Test Sections

Details of the test sections and turbulators can be found in Fig. 1 and Table 1. A liquid crystal technique[11] was employed to measure the heat transfer coefficients in these test sections. In this technique, the most temperature-sensitive color displayed by the liquid crystals is chosen as the reference color corresponding to a known temperature. By proper adjustment of the Ohmic power to a heater immediately underneath the liquid crystals, the reference color is moved from one location to another such that the entire area of interest is eventually covered with the reference color at one time or another. This process results in a series of photographs each corresponding to a certain location of the reference color. Knowing the heat flux, the surface temperature, and the air mixed mean temperature, one can calculate the heat transfer coefficient associated with each photograph. The air mixed mean temperature is calculated through an energy balance between the test section inlet and the location of the camera. The area covered by the reference color in each photograph is then digitized to be used for an area-weighted average heat transfer coefficient calculation.

All test sections, 46 in. in length, were rectangular channels, three walls of which were made of 0.5-in.-thick clear acrylic. The fourth wall, on which the heaters and liquid crystal sheets were attached and all measurements were taken, was made of a 2-in.-thick machineable polyurethane slab. This wall, for all cases tested, had a fixed width of 3 in. Thus, any variation of test section aspect ratio was accomplished by varying the width of its two adjacent acrylic walls. Depending on the turbulator pitch, approximately 32 in. of the test section length was turbulated, leaving about 14 in. of all-smooth walls at the entrance of the test section. This simulates the unturbulated cooling passage in the dovetail region of an airfoil. Heat transfer measurements were performed for an area between a pair of turbulators in the middle of the turbulated zone corresponding to an X/D_h of about 16 from the test section entrance. Turbulators were also machined out of clear acrylic and glued onto two opposite walls in a staggered arrangement. Four 3- × 11-in. custom-made etched-foil heaters with a thickness of 0.006 in. were placed on the polyurethane wall where measurements were taken using a special double-stick 0.002-in.-thick tape with minimal temperature deformation. The heaters covered the entire test section length including the nonturbulated entry length. However, they did not extend over the actual turbulator surface. It is noted that an experimental investigation by El-Husayni et al.[12] on heat transfer in a turbulated channel with one, two, and four heated walls showed that, in a stationary turbulated channel, the heat transfer coefficient is not sensitive to the choice of wall thermal boundary conditions. The 0.005-in.-thick liquid crystal foil was then placed on the heaters. Static pressure taps were mounted on all four walls of each test section to measure the pressure drop across the test section. The reported $\bar{f}$ is the overall average for all four walls.

The test sections were covered on all sides, except for a small window at the location where the pictures were taken, by 2-in.-thick insulation slabs to minimize heat losses to the environment. The radiational heat loss from the heated wall to the unheated walls, as well as the losses to the ambient air, were taken into consideration when heat transfer coefficients were calculated.

A 35-mm, programmable camera in conjunction with proper filters and background lighting to simulate daylight condi-

tions, were used to take photographs of isochrome patterns formed on the liquid crystal sheet. Surface heat flux in the test section was generated by the heaters through a custom-designed power supply unit. Each heater was individually controlled by a variable transformer.

Procedure

At the beginning of the set of test runs the liquid crystal sheets were calibrated. A water bath was used to attain uniform isochromes on a small piece of the liquid crystal sheet used throughout this investigation. The temperature corresponding to each color was measured using a precision thermocouple, and photographs were taken at laboratory conditions simultaneously so as to simulate closely the actual testing environment. A reference color then was chosen to be used throughout the experiments. In a typical test run, the Reynolds number was set by precisely fixing the mass flow rate. Heat flux was induced by turning on the main power supply and adjusting each heater's power individually until the first band of reference color was observed on the liquid crystal sheet in the area of interest. Enough time was given so that the system came to thermal equilibrium at which time a photograph was taken and data recorded. The power to the heaters was then increased such that the reference color was moved to a location next to the previous one and another picture was taken. This procedure was continued until eventually the whole area between a pair of turbulators was covered by the reference color at one time or another. The process was repeated for all Reynolds numbers.

The next step was to digitize each picture to measure the area covered by the reference color. This was done by using a magnetic tablet and a commercial software package installed on an IBM AT PC. Once the areas were measured, an area-weighted average heat transfer coefficient was calculated.

For verification of the liquid crystal technique accuracy, an all-smooth-wall channel was tested first. The results which were within ±5% of the well-known Dittus-Boelter[13] correlation are reported in Taslim.[14] Furthermore, these authors' previous results of turbulated channels of various geometries using the same technique compared favorably with those of other investigators.[15]

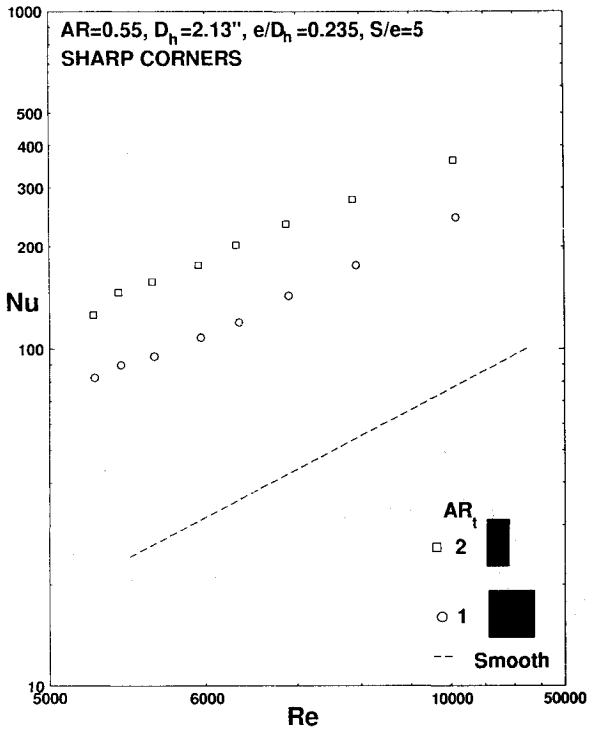

Fig. 2 Effects of turbulator aspect ratio on Nusselt number.

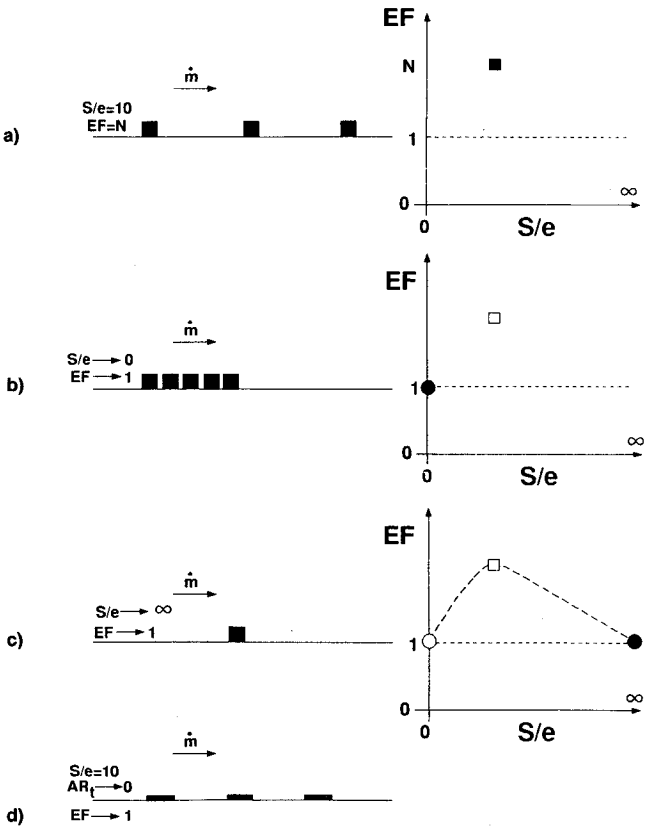

Fig. 3 Conceptual relationship between turbulator spacing S/e and aspect ratio AR_t. Typical enhancement factors when a) $S/e = 10$, b) $S/e \rightarrow 0$, c) $S/e \rightarrow \infty$, and d) $AR_t \rightarrow 0$.

Experimental uncertainties, following the method of Kline and McClintock,[16] were determined to be ±6 and ±8% for the heat transfer coefficient and friction factor, respectively.

Results and Discussion

As dimensions for small turbulated airfoils decrease, it becomes increasingly more difficult to cast turbulators with aspect ratios above unity because of the previously mentioned nonfill problem. An obvious solution to avoid nonfill is to lower AR_t, thereby reducing the groove depth on the casting core into which the molten metal has to flow. The negative effect of decreasing AR_t on heat transfer coefficient is seen in Fig. 2 where it is shown that as AR_t is decreased from 2 to 1, a 33% decrease in Nu occurs for high blockage ratio turbulators ($e/D_h = 0.235$) at a spacing, S/e, of 5. In most cases a 33% reduction in Nu would be unacceptable and, therefore, some other solution is required. It is not anticipated, however, that a decrease of this magnitude will occur for all combinations of S/e and e/D_h. For all figures in which Nusselt number is plotted vs Reynolds number, the dashed line, corresponding to the all-smooth-wall case, is the well-known Dittus-Boelter correlation given by $Nu_s = 0.023Re^{0.8}Pr^{0.4}$. In Fig. 3 the rationale of an optimum S/e with respect to heat transfer behavior is developed. It has been established both experimentally and analytically that, given enough space between a pair of turbulators for the flow to reattach, the heat transfer coefficient reaches its maximum in the reattachment zone and decreases monotonically in the flow direction until it approaches the next turbulator where it starts to increase again due to a stagnation point type of flow. Therefore, intuitively, decreasing the flow length from the reattachment zone to the next turbulator should increase the overall heat transfer coefficient for the surface area between a pair of turbulators. If the total distance between a pair of turbulators is decreased too much, there will not be sufficient length for the flow to

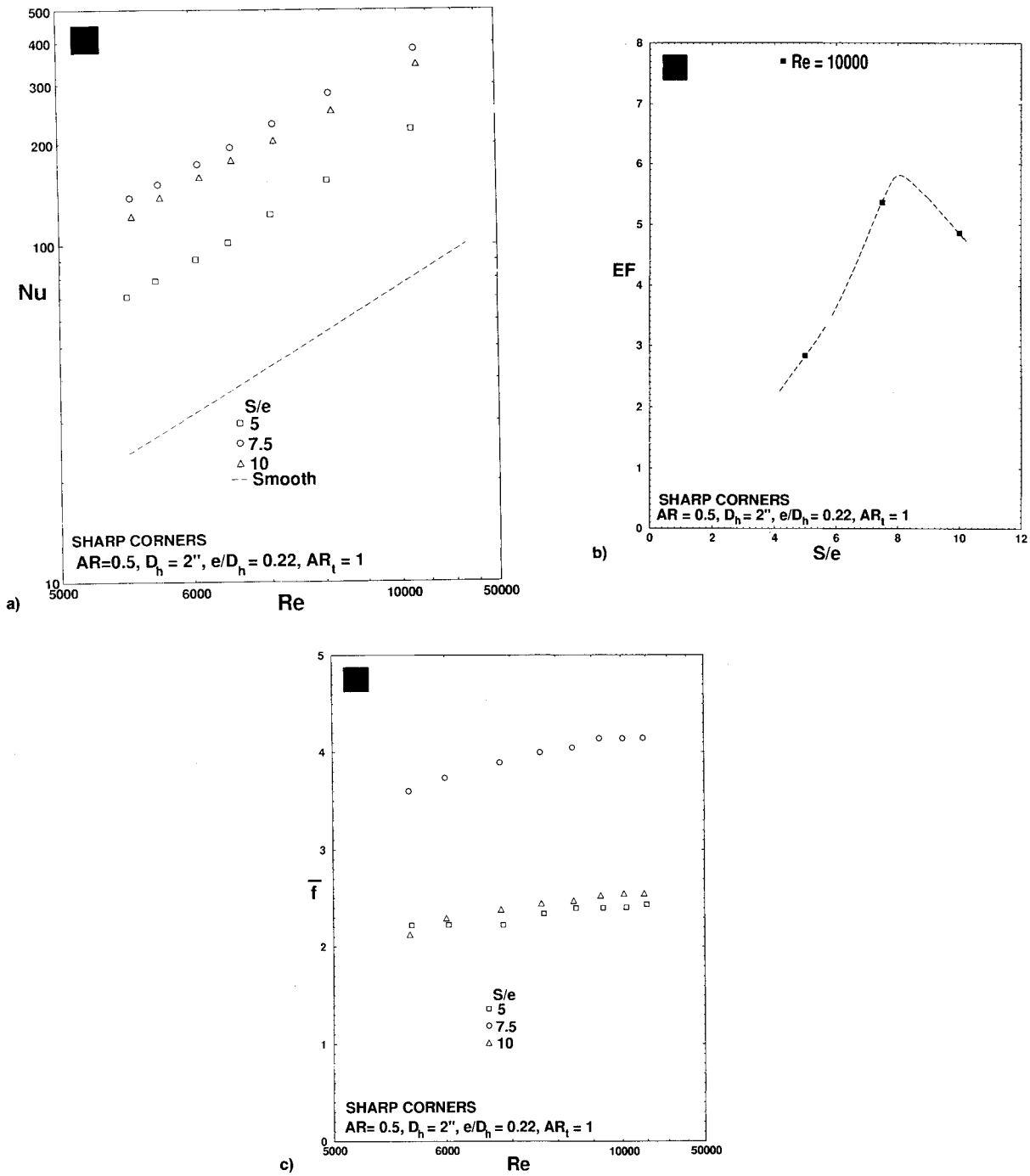

Fig. 4 Effect of *S/e* on the heat transfer coefficient and the friction factor.

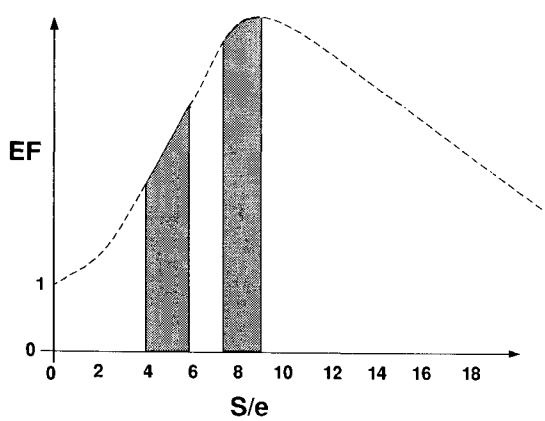

Fig. 5 Conceptual *EF* sensitivity to *S/e*.

reattach, and thus, the region of maximum heat transfer coefficient is lost. Figure 3 further illustrates the rationale of an optimum *S/e* with respect to heat transfer coefficient. Figure 3a shows a turbulated wall at an assumed optimum spacing with its corresponding $EF = Nu/Nu_s$. In Fig. 3b, as *S/e* approaches the lower limit of 0, *EF* must approach that of a smooth wall, $EF = 1$ with a smaller D_h. In Fig. 3c, as *S/e* approaches infinity, the overall average *EF* for the surface between turbulators once again approaches that of a smooth wall. Clearly, there exists a point between 0 and ∞ where *S/e* would be optimum from a heat transfer point of view. Previous investigations[17] have shown that for blockage ratios below 0.1 the optimum *S/e* occurs between 7–11. Figure 3d shows that there is a similar relationship between turbulator spacing (*S/e*) and aspect ratio (AR_t) when considering their effects on heat transfer behavior. In Fig. 3d, the turbulator arrangement starts out as an optimum as in Fig. 3a. The

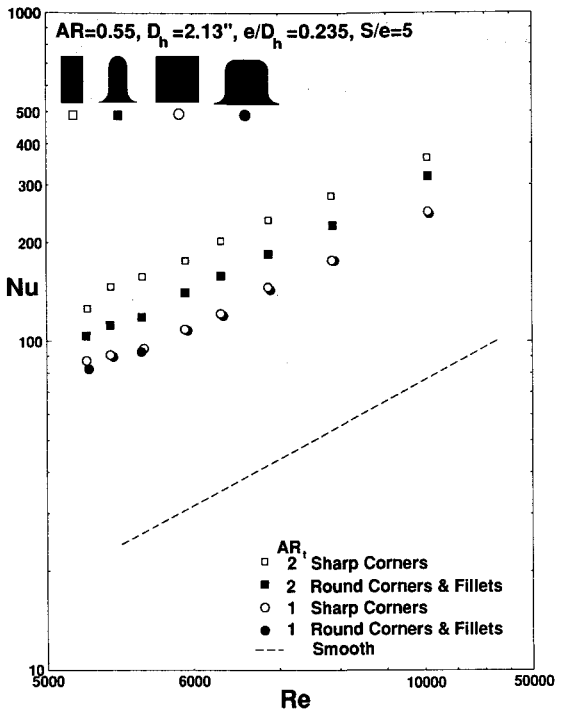

Fig. 6 Effects of fillets and corner radii on the heat transfer coefficient.

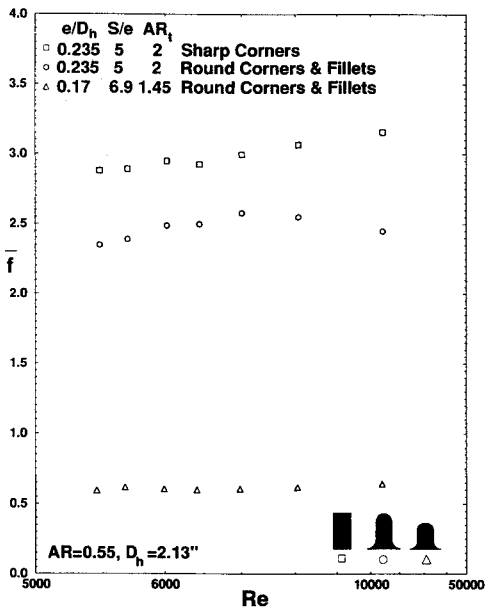

Fig. 7 Effects of fillets and corner radii on the friction factor.

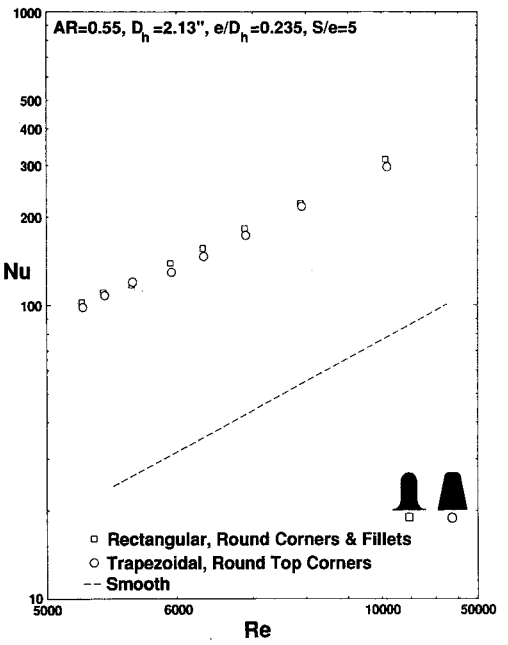

Fig. 8 Trapezoidal-shape vs high-aspect-ratio turbulators.

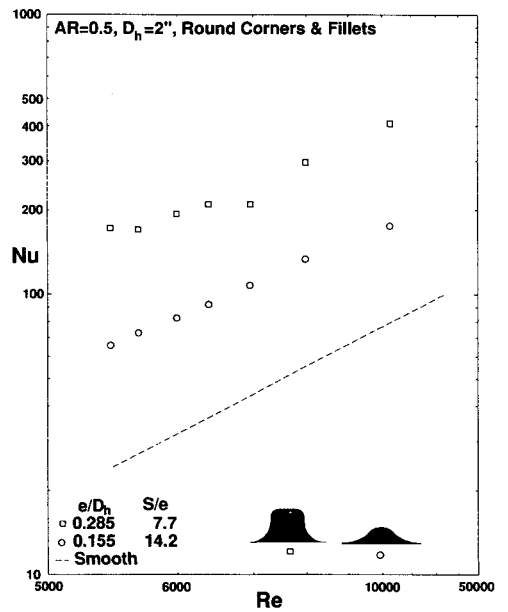

Fig. 9 Effects of max/min tolerances on the heat transfer coefficient for $S/e = 10$.

turbulator aspect ratio is then allowed to approach its limit of 0, and again its EF must approach that of a smooth wall as occurs in Fig. 3b (for $S/e \rightarrow 0$). Thus, allowing $AR_t \rightarrow 0$ has a similar effect on EF as allowing $S/e \rightarrow 0$.

Figures 4a and 4b show that for a square turbulator with a relatively high blockage ratio ($e/D_h = 0.22$), the optimum appears to be around 8. Zhang et al.[18] have reported the same optimum value for a combination of 90-deg low blockage ratio turbulators and grooves. In addition to a region of optimum S/e, Fig. 4 illustrates a much higher degree of sensitivity to S/e than has been observed for low blockage ratio turbulators ($e/D_h \leq 0.1$). Figure 4c shows the same behavior for the friction factor.

Having developed the relationship between AR_t and S/e, the large difference in Nu for the two tested geometries in Fig. 2 can be explained. Figure 5 once again shows an EF vs S/e optimization curve. Turbulators designed to the optimum S/e will have EF located on the flat (less sensitive) part of the curve. Turbulators located away from the optimum (as is the case for turbulators in Fig. 2 where $S/e = 5$) will have EF located on the more sensitive part of the curve. Here, it is shown that nonoptimum S/e will be much more sensitive to changes in S/e or AR_t (based on similarity) than those designed to an optimum S/e.

The geometries tested in Fig. 2 are idealistic with respect to their sharp-edged tip and fillet radii. It is expected that as these sharp corners become more rounded, EF will decrease. Figure 6 shows the effect on Nu of the geometries tested in Fig. 2 when realistic manufacturing limits are imposed. It is seen that while the effect of rounding decreases Nu for both geometries, the higher aspect ratio turbulator ($AR_t = 2$) is more sensitive to the rounding effects with a 17% reduction than the lower aspect ratio turbulator ($AR_t = 1$) with a 5%

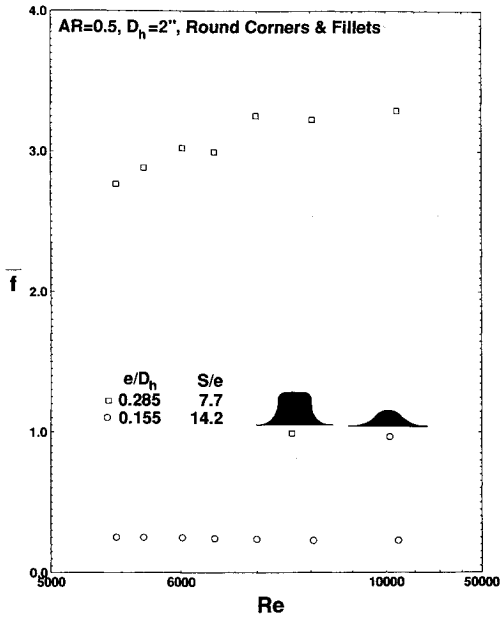

Fig. 10 Effects of max/min tolerances on the friction factor for S/e = 10.

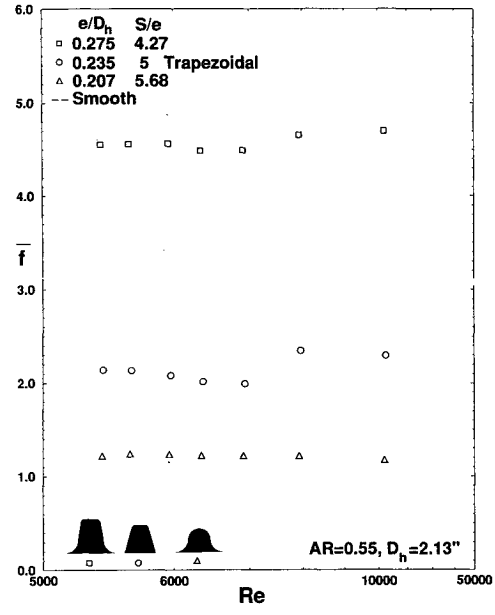

Fig. 12 Effects of max/min tolerances on the friction factor for S/e = 5.

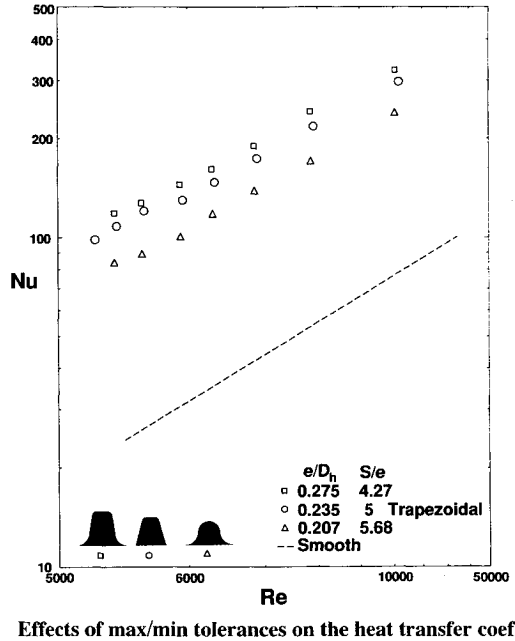

Fig. 11 Effects of max/min tolerances on the heat transfer coefficient for S/e = 5.

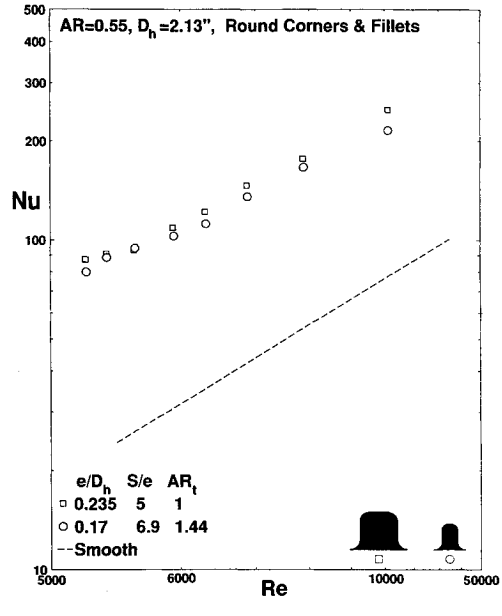

Fig. 13 Optimization through turbulator S/e and AR_t.

reduction. The effect that round edges and fillets have on the friction factor for high aspect ratio turbulators is shown in Fig. 7. The effect is much more pronounced than the case of square or low aspect ratio turbulators that are to be presented shortly. For geometries presented in Fig. 6, although at the same S/e, the distance between turbulator sidewalls is different due to the differences in AR_t. The higher AR_t geometry provides more space between turbulators for the flow to reattach to the surface within the turbulator sidewalls, thus allowing more sensitivity to the rounded turbulator profile. The lower AR_t geometry does not provide sufficient space between turbulators for the flow to reattach, resulting in tip-to-tip turbulator flow, and hence, it reduces the sensitivity to turbulator profile. From this, a turbulator design that shows both enhanced castability while maintaining heat transfer performance can be envisioned. For this spacing (S/e = 5), where flow is sensitive to tip width, the turbulator tip width needs to remain small. To ease castability, the turbulator base width needs to remain large. The resultant turbulator would be trapezoidal in shape. Figure 8 shows the Nu for a trapezoidal-shaped turbulator at S/e = 5 is nearly the same as for a rectangular turbulator with an AR_t = 2 at the same spacing.

In small airfoils the effect of manufacturing tolerances on turbulator profiles can be significant. A typical minimum nominal height for a cast turbulator is 0.010 in., with a minimum tolerance of ±0.003 in. For small airfoils, a 0.010-in.-high turbulator could represent a high blockage ratio. It has been established in previous investigations[19,20] that EF become increasingly more sensitive to blockage ratio as blockage ratio increases. For a high turbulator blockage ratio airfoil design with turbulator heights of 0.010 ± 0.003 in., the blockage ratio could change by ±30%. For this case, the effect on passage Nu of max/min tolerance must be known so that accurate airfoil temperatures, and ultimately life limits, can be predicted.

Figure 9 shows the deviation in Nu due to geometric tolerances for a turbulated passage with a nominal turbulator height of 0.010 in. and a ±0.003-in. tolerance. For this case the nominal blockage and spacing ratios are 0.22 and 10, respectively, resulting in a maximum e/D_h = 0.285 with a corresponding S/e = 7.7, and a minimum e/D_h = 0.155 cor-

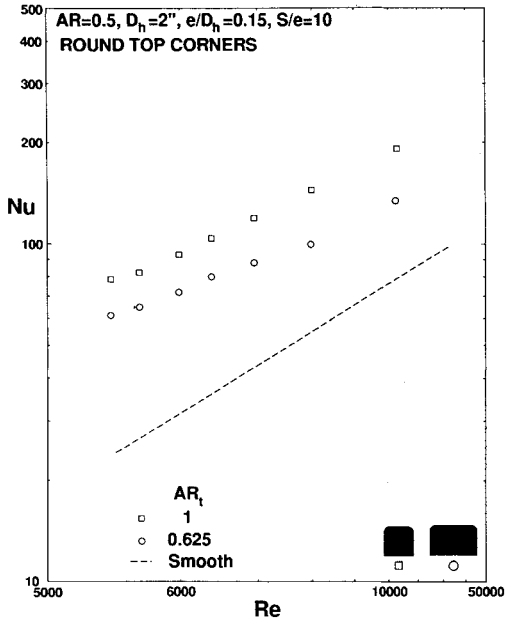

Fig. 14 Heat transfer performance of square vs low aspect ratio turbulators.

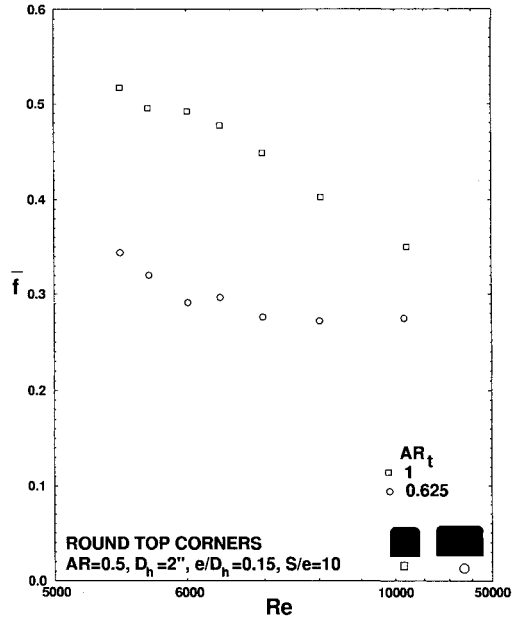

Fig. 15 Friction factor for square vs low aspect ratio turbulators.

responding to $S/e = 14.2$. The results show that a $\pm 40\%$ deviation in Nu from the arithmetic max/min average for this design can be expected due to manufacturing tolerances alone. Variation in friction factor is shown in Fig. 10. The turbulator profiles shown in Fig. 9 are representative of the max/min profiles that would occur within the tolerance envelope. For airfoils where geometries such as this occur, it becomes obvious that analysis must be made at max/min conditions and careful monitoring of tolerances are required.

Figures 11 and 12 show the variation in Nu and friction factor due to manufacturing tolerances for a nominal trapezoidal-shaped turbulator ($e/D_h = 0.235$, $S/e = 5$). For this case, the turbulator height was allowed to vary $\pm 15\%$. It is seen that the variation in Nu from the nominal case is $+22\%$ and -13% from max/min profiles, respectively. Although not isolated specifically, it should be remembered that there are three separate geometrical effects on the deviation in EF from the nominal to maximum or minimum, specifically: e/D_h, S/e, and turbulator profile. Figure 13 further demonstrates the strong effect S/e and AR_t have on Nu. Here, the turbulator ($AR_t = 1$, rounded corners) from Fig. 5 is compared to a turbulator with decreased e/D_h, but increased S/e and AR_t. The results show that the decrease in Nu due to the decrease in e/D_h from 0.235 to 0.17 is completely offset by the increase in AR_t from 1 to 1.44, and by increasing S/e from the relatively low value of 5 towards a more optimum of 6.9.

Figures 14 and 15 show the effect on Nu and friction factor of turbulator aspect ratio for a spacing of 10. For this case, the turbulator blockage ratios, while not low, are a more moderate 0.15. AR_t is decreased from 1.0 to 0.625 with a resulting decrease in Nu of 22% (at $Re = 10^4$). The sensitivity of both Nu and friction factor to AR_t for this case is less than the case in Fig. 2. This is consistent with the $S/e - AR_t$ relationship developed in Figs. 3 and 4, whereas the sensitivity should be decreased because the S/e is closer to the optimum value and the blockage ratios are at a lower-less sensitive value.

Conclusions

A parametric investigation was performed to experimentally determine what effects turbulator spacing and profile have on heat transfer coefficients in small cooled turbine airfoils. Since these parameters are largely dependent upon current manufacturing limitations, a better understanding of their effects will facilitate more producible cooled airfoil designs. The results indicate the following:

1) There exists an optimum turbulator spacing S/e for every given turbulator blockage ratio e/D_h and aspect ratio AR_t. The sensitivity of Nu to S/e decreases as e/D_h decreases.

2) Nusselt numbers decrease as AR_t decreases. Nusselt numbers are more sensitive to a decrease in AR_t as S/e decreases below the optimum value.

3) There exists a similarity relationship between S/e and AR_t such that for a given S/e, as $AR_t \rightarrow 0$, heat transfer coefficient approaches that of a smooth passage similarly as when $S/e \rightarrow 0$.

4) For a nonoptimum spacing ($S/e = 5$) a trapezoidal-shaped turbulator enhances the castability of the turbulator by providing a wider turbulator base, thus decreasing the possibility of nonfill, while maintaining the same heat transfer performance as a large aspect ratio turbulator.

5) Effects on heat transfer coefficients in small airfoils due to turbulator manufacturing tolerances are significant and must be accounted for when airfoil temperatures are predicted.

References

[1]Burggraff, F., "Experimental Heat Transfer and Pressure Drop with Two Dimensional Turbulence Promoters Applied to Two Opposite Walls of a Square Tube," *Augmentation of Convective Heat and Mass Transfer*, edited by A. E. Bergles and R. L. Webb, American Society of Mechanical Engineers, New York, 1970, pp. 70–79.

[2]Chandra, P. R., and Han, J. C., "Pressure Drop and Mass Transfer in Two-Pass Ribbed Channels," *Journal of Thermophysics and Heat Transfer*, Vol. 3, No. 3, 1989, pp. 315–319.

[3]Chandra, P. R., "Effect of Rib Angle on Local Heat/Mass Transfer Distribution in a Two Pass Rib-Roughened Channel," American Society of Mechanical Engineers Paper 87-GT-94, June 1987.

[4]Han, J. C., Glicksman, L. R., and Rohsenow, W. M., "An Investigation of Heat-Transfer and Friction for Rib Roughened Surfaces," *International Journal of Heat and Mass Transfer*, Vol. 21, 1978, pp. 1143–1156.

[5]Han, J. C., "Heat Transfer and Friction in Channels with Two Opposite Rib-Roughened Walls," *Journal of Heat Transfer*, Vol. 106, No. 4, 1984, pp. 774–781.

[6]Han, J. C., Park, J. S., and Lei, C. K., "Heat Transfer Enhancement in Channels with Turbulence Promoters," *Journal of Engineering for Gas Turbines and Power*, Vol. 107, No. 1, 1985, pp. 628–635.

[7]Mayle, R. E., "Pressure Loss and Heat Transfer in Channels Roughened on Two Opposed Walls," *Journal of Turbomachinery*, Vol. 113, No. 1, 1991, pp. 60–66.

[8]Metzger, D. E., Fan, C. S., and Pennington, J. W., "Heat Transfer and Flow Friction Characteristics of Very Rough Transverse Ribbed

Surfaces with and Without Pin Fins," *Proceedings of the ASME-JSME Thermal Engineering Joint Conference*, Vol. 1, ASME, New York, 1983, pp. 429–436.

[9]Taslim, M. E., and Spring, S. D., "An Experimental Investigation of Heat Transfer Coefficients and Friction Factors in Passages of Different Aspect Ratios Roughened with 45° Turbulators," *Proceedings of the ASME National Heat Conference* (Houston, TX), ASME, New York, 1988.

[10]Taslim, M. E., and Spring, S. D., "Experimental Heat Transfer and Friction Factors in Turbulated Cooling Passages of Different Aspect Ratios, Where Turbulators are Staggered," AIAA Paper 88-3014, July 1988.

[11]Simonich, J. C., and Moffat, R. J., "New Technique for Mapping Heat Transfer Coefficient Contours," *Review of Scientific Instruments*, Vol. 53, No. 5, 1982, pp. 678–683.

[12]El-Husayni, H. A., Taslim, M. E., and Kercher, D. M., "Experimental Heat Transfer Investigation of Stationary and Orthogonally Rotating Asymmetric and Symmetric Heated Smooth and Turbulated Channels," *Journal of Turbomachinery*, Vol. 116, No. 1, 1994, pp. 124–132.

[13]Dittus, F. W., and Boelter, L. M. K., *Publications in Engineering*, Vol. 2, No. 13, Univ. of California, Berkeley, CA, 1930, pp. 443–461.

[14]Taslim, M. E., "Application of Liquid Crystals in Heat Transfer Coefficient Measurement," *Proceedings of the ELECTRO®/90 Conference Record*, sponsored by Region 1, Central New England Council, METSAC, IEEE, and New England and New York Chapters, ERA, Boston, MA, 1990, pp. 274–282.

[15]Taslim, M. E., Bondi, L. A., and Kercher, D. M., "An Experimental Investigation of Heat Transfer in an Orthogonally Rotating Channel Roughened with 45 Degree Criss-Cross Ribs on Two Opposite Walls," *Journal of Turbomachinery*, Vol. 113, No. 3, 1990, pp. 346–353.

[16]Kline, S. J., and McClintock, F. A., "Describing Uncertainty in Single-Sample Experiments," *Mechanical Engineering*, Vol. 75, Jan. 1953, pp. 3–8.

[17]Webb, R. L., Eckert, E. R. G., and Goldstein, R. J., "Heat Transfer and Friction in Tubes with Repeated-Rib-Roughness," *International Journal of Heat and Mass Transfer*, Vol. 14, 1971, pp. 601–617.

[18]Zhang, Y. M., Gu, W. Z., and Han, J. C., "Heat Transfer and Friction in Rectangular Channels with Ribbed or Ribbed-Grooved Walls," *Journal of Heat Transfer*, Vol. 116, No. 1, 1994, pp. 58–65.

[19]Taslim, M. E., Rahman, A., and Spring, S. D., "An Experimental Investigation of Heat Transfer Coefficients in a Spanwise Rotating Channel with Two Opposite Rib-Roughened Walls," *Journal of Turbomachinery*, Vol. 113, No. 1, 1991, pp. 75–82.

[20]Taslim, M. E., and Spring, S. D., "Friction Factors and Heat Transfer Coefficients in Turbulated Cooling Passages of Different Aspect Ratios, Part I: Experimental Results," AIAA Paper 87-2009, July 1987.